REPORT DOCUMENTATION PAGE

The public reporting burden for this collection of information is estimated to average 1 hour per response, including the time for reviewing instructions, searching existing data sources, gathering and maintaining the data needed, and completing and reviewing the collection of information. Send comments regarding this burden estimate or any other aspect of this collection of information, including suggestions for reducing the burden to Department of Defense, Washington Headquarters Services Directorate for Information Operations and Reports (0704-0188), 1215 Jefferson Davis Highway, Suite 1204, Arlington VA 22202-4302. Respondents should be aware that notwithstanding any other provision of law, no person shall be subject to any penalty for failing to comply with a collection of information if it does not display a currently valid OMB control number.
PLEASE DO NOT RETURN YOUR FORM TO THE ABOVE ADDRESS.

1. REPORT DATE (DD-MM-YYYY)	2. REPORT TYPE	3. DATES COVERED (From - To)
10-08-2009	REPRINT	

4. TITLE AND SUBTITLE
A Comparison of Elemental Abundance Ratios in SEP Events in Fast and Slow Solar Wind Regions

5a. CONTRACT NUMBER

5b. GRANT NUMBER

5c. PROGRAM ELEMENT NUMBER
62601F

6. AUTHORS
S. W. Kahler
A. J. Tylka*
D. V. Reames**

5d. PROJECT NUMBER
2301

5e. TASK NUMBER
RD

5f. WORK UNIT NUMBER
Z4

7. PERFORMING ORGANIZATION NAME(S) AND ADDRESS(ES)

Air Force Research Laboratory /RVBXS
29 Randolph Road
Hanscom AFB, MA 01731-3010

8. PERFORMING ORGANIZATION REPORT NUMBER

AFRL-RV-HA-TR-2009-1133

9. SPONSORING/MONITORING AGENCY NAME(S) AND ADDRESS(ES)

10. SPONSOR/MONITOR'S ACRONYM(S)
AFRL/RVBXS

SPONSOR/MONITOR'S REPORT

20100315120

12. DISTRIBUTION/AVAILABILITY STATEMENT
Approved for Public Release; distribution unlimited.

14. ABSTRACT

The solar energetic ($E > 1$ MeV nucleon^{-1}) particles (SEPs) observed in gradual events at 1 AU are assumed to be accelerated by coronal/interplanetary shocks from ambient thermal or suprathermal seed particles. If so, then the elemental abundances of SEPs produced in different solar win (SW) stream types (transient, fast, and slow) might be systematically distinguished from each other. We look for these differences in SEP energy spectra and in elemental abundance ratios (including Mg/Ne and Fe/C, which compare low/high first ionization potential elements), in a large number of SEP time intervals over the past solar cycle. The SW regions are characterized by the three-component stream classification of Richardson et al. Our survey shows no significant compositional or energy spectral differences in the 5-10 MeV nucleon^{-1} range for SEP events of different SW stream types. This result extends the earlier finding that SEP events are observed frequently in fast SW streams, although their higher Alfven and SW flow speeds should constrain SEP production by coronal mass ejection-driven shocks in those regions. We discuss the implications of our results for shock seed populations and cross-field propagation.

15. SUBJECT TERMS

Acceleration of particles	Solar wind	Sun:abundances	Sun:coronal mass ejections

16. SECURITY CLASSIFICATION OF:

a. REPORT	b. ABSTRACT	c. THIS PAGE	17. LIMITATION OF ABSTRACT	18. NUMBER OF PAGES	19a. NAME OF RESPONSIBLE PERSON
UNCL	UNCL	UNCL	UNL		S. W. Kahler

19B. TELEPHONE NUMBER (Include area code)

A COMPARISON OF ELEMENTAL ABUNDANCE RATIOS IN SEP EVENTS IN FAST AND SLOW SOLAR WIND REGIONS

S. W. KAHLER[1], A. J. TYLKA[2], AND D. V. REAMES[3]

[1] Air Force Research Laboratory, RVBXS, 29 Randolph Road, Hanscom AFB, MA 01731, USA; AFRL.RVB.PA@hanscom.af.mil
[2] Space Science Division, Naval Research Laboratory, Washington, DC 20375, USA
[3] Institute for Physical Science and Technology, University of Maryland, College Park, MD 20742, USA

ABSTRACT

The solar energetic ($E > 1$ MeV nucleon^{-1}) particles (SEPs) observed in gradual events at 1 AU are assumed to be accelerated by coronal/interplanetary shocks from ambient thermal or suprathermal seed particles. If so, then the elemental abundances of SEPs produced in different solar wind (SW) stream types (transient, fast, and slow) might be systematically distinguished from each other. We look for these differences in SEP energy spectra and in elemental abundance ratios (including Mg/Ne and Fe/C, which compare low/high first ionization potential elements), in a large number of SEP time intervals over the past solar cycle. The SW regions are characterized by the three-component stream classification of Richardson et al. Our survey shows no significant compositional or energy spectral differences in the 5–10 MeV nucleon^{-1} range for SEP events of different SW stream types. This result extends the earlier finding that SEP events are observed frequently in fast SW streams, although their higher Alfven and SW flow speeds should constrain SEP production by coronal mass ejection-driven shocks in those regions. We discuss the implications of our results for shock seed populations and cross-field propagation.

Key words: acceleration of particles – solar wind – Sun: abundances – Sun: coronal mass ejections (CMEs) – Sun: particle emission

1. INTRODUCTION

Gradual solar energetic ($E > 1$ MeV nucleon^{-1}) particle (SEP) events observed at 1 AU are understood to be produced in coronal/interplanetary magnetohydrodynamics (MHD) shocks driven by fast coronal mass ejections (CMEs) (e.g., Reames 1999; Tylka & Lee 2006; Lee 2007). Fast CMEs are observed to precede every gradual SEP event, but attempts to correlate CME properties, speeds in particular, with SEP intensities (Kahler 2001) or timescales (Kahler 2005) at 1 AU have been only moderately successful. It is clear that the coronal/ interplanetary environment into which a fast CME propagates must be a significant factor for the production of a shock and subsequent shock acceleration of thermal or suprathermal ions to SEPs. Kahler & Reames (2003) suggested that SEP production might be more restricted in fast solar wind (SW) streams compared with slow SW streams because both the MHD fast-mode speeds and the SW flow speeds v_{sw} are higher and therefore less favorable for shock acceleration in the fast SW streams. Furthermore, if ions in the suprathermal tails of speed distributions extending to $\gtrsim 10 \times v_{sw}$ are the SEP seed populations (Lee 2007), then the much weaker tails observed in the fast SW regions (Gloeckler 2003) should further limit SEP production in those regions (Kahler 2004).

Several studies have found no characteristic differences between SEP events in fast and slow SW regions. Kahler (2004) compared 20 MeV SEP events in fast and slow SW regions defined by SW O^{+7}/O^{+6} ratios and found not only that SEP events occurred commonly in fast SW regions, but that their 20 MeV peak intensities and associated CME speeds matched those SEP events observed in slow SW regions. In addition, Kahler (2005, 2008) found no dependence of any SEP event timescales, such as rise times or durations, on SW stream type.

These results suggest two possibilities. First, SEPs may be accelerated preferentially in slow SW regions but propagate broadly in longitude and populate the fast SW regions at 1 AU. Either the supradiffusive transport of magnetic field lines across the main Parker spiral field directions (Ragot 2006) or cross-field transport of the SEPs could produce this propagation effect. The second possibility is that SEPs may be accelerated in both kinds of SW regions. In the latter case, we might expect to find SEP elemental abundance variations at 1 AU reflecting the stream differences in shock seed populations or in shock structures (Kahler 2004; Tylka et al. 2005). Elemental abundances of SW stream ions have been compared with those of SEPs (Mewaldt et al. 2006, 2007a), but no comparison of SEP abundances between fast and slow SW has been done to search for evidence of SW-stream differences in shocks or in seed populations.

Here, we review SEP and SW elemental abundances and consider candidate seed populations of shock acceleration to determine expected SEP elemental abundances in fast and slow SW. We then survey gradual SEP events to look for any abundance dependence on the type of ambient SW. Since shock fractionation also plays a role in forming SEP energy spectra (Mewaldt et al. 2005; Tylka & Lee 2006; Lee 2007), and in weak shocks those spectra reflect the suprathermal seed spectra of the SW streams, we also examine the SEP elemental energy spectra in the different kinds of SW.

2. SEP AND SW ELEMENTAL ABUNDANCES

2.1. Gradual SEP Abundances

The standard set of gradual SEP elemental abundances is that of Reames (1995, 1999), which we reproduce in Table 1 for the most abundant elements. The abundances of event fluences are normalized to $O = 1000$ and are derived at 5–12 MeV nucleon^{-1} except for H and He, which were derived at 1 MeV nucleon^{-1}.

Table 1
Solar, SEP, and SW Elemental Abundances

Element	FIP (e.V.)	Z	Photospheric	Gradual SEP Events[b]	Coronal Above AR	Solar Wind Slow[c]	Solar Wind Fast[c]	*Ulysses* Fast[d]
H[a]	13.60	01	$(2.04 \pm -)(6)$	$1.57 \pm 0.22(6)$	1.48(6)	—	—	—
He[a]	24.59	02	$1.618 \pm 0.037(5)$	$57 \pm 3(3)$	1.26(5)	$(90 \pm 30)(3)$	$(75 \pm 10)(3)$	—
C	11.26	06	501 ± 47	465 ± 9	490	680 ± 70	680 ± 70	710 ± 80
N	14.53	07	138 ± 35	124 ± 3	123	78 ± 5	114 ± 21	143 ± 16
O	13.62	08	1000 ± 115	1000 ± 10	1000	1000	1000	1000
Ne	21.56	10	151 ± 35	152 ± 4	191	140 ± 30	140 ± 30	71 ± 10
Na	5.14	11	4.07 ± 0.28	10.4 ± 1.1	12.3	9.0 ± 1.5	5.1 ± 1.4	—
Mg	7.65	12	72.4 ± 3.3	196 ± 4	224	147 ± 50	106 ± 50	108 ± 22
Al	5.99	13	5.89 ± 0.27	15.7 ± 1.6	18.2	11.9 ± 3	8.1 ± 0.4	—
Si	8.15	14	70.8 ± 3.2	152 ± 4	214	140 ± 50	101 ± 40	88 ± 14
S	10.36	16	31.6 ± 0.3	31.8 ± 0.7	31.6	50 ± 15	50 ± 15	35 ± 4
Ar	15.76	18	7.24 ± 1.34	3.3 ± 0.2	5.75	3.1 ± 0.8	3.1 ± 0.4	1.8 ± 0.4
Ca	6.11	20	4.47 ± 0.31	10.6 ± 0.4	13.2	8.1 ± 1.5	5.3 ± 1.0	7 ± 3
Cr	6.77	24	0.91 ± 0.10	2.1 ± 0.3	$\cdots$	2.0 ± 0.3	1.5 ± 0.3	—
Fe	7.90	26	60.3 ± 4.1	$134. \pm 4$	186	122 ± 50	88 ± 50	67 ± 7
Ni	7.64	28	3.39 ± 0.23	6.4 ± 0.6	10.5	—	—	—

Notes.

[a] Quantities for H and He in parentheses are powers of 10 (6 is 10^6)

[b] Error bars are statistical uncertainties in the mean values.

[c] According to Bochsler (2007), these "uncertainties have been estimated from statistical fluctuations to the one-sigma level but do also include systematic uncertainties."

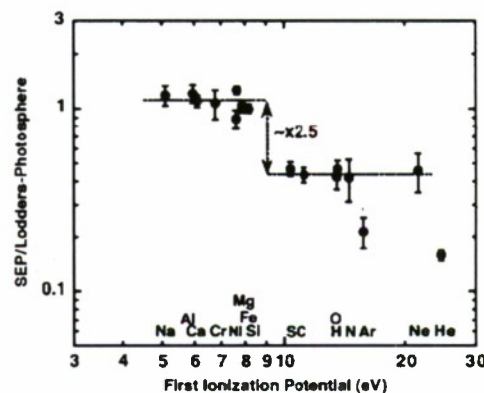[d] According to Gloeckler & Geiss (2007), these "errors are mostly systematic."

SEP abundances are energy dependent (Reames 1999), but variations among SEP events in the energy spectral shapes and in the derived abundances are generally smaller at low ($\sim$1 MeV nucleon^{-1}) than at high (> 10 MeV nucleon^{-1}) energies (Mazur et al. 1992). Shock diffusion theory predicts that particle escape from shocks also increases with energy, leading to enhanced abundance variations with energy (Reames 1995). The energy dependence of Fe/O ratios reported by different studies can be seen in Figure 6 of Desai et al. (2006c).

2.2. SEP Seed Particle Populations

2.2.1. Coronal Thermal Ions as Seeds

Reames (1995, 1999) argued that the elemental abundances of gradual SEP events reflect the composition of the solar corona, implying that the ambient coronal thermal ions, which are the source of the SW, constitute the seed particles of the gradual SEP events. The seed population abundance was well reflected and in good agreement with coronal abundances at low ($\sim$5 MeV nucleon^{-1} for $Z > 2$ and 1–4 MeV nucleon^{-1} for H and He) energies (Reames 1995). We will use similar energy ranges in this study, for which the Low Energy Matrix Telescope (LEMT; von Rosenvinge et al. 1995) instrument on *Wind* offers the most sensitive, precise, and extensive SEP elemental measurements ever achieved.

If coronal material is the source of both the SW and the seed population of gradual SEPs, the SW relative abundances should match those of the gradual SEPs. Mewaldt et al. (2001) compared the SW elemental abundances of von Steiger et al. (2000) with those in gradual SEP events (Reames 1998) and questioned the basic assumption that coronal thermal ions are the seed population for the SEP events. They noted that the ratio by which the abundances of elements with high ($\gtrsim$9 eV) first ionization potential (FIP) are depleted relative to those of low ($\lesssim$9 eV) FIP in comparison to photospheric abundances (Figure 1), is much less in both slow ($\sim$2.4) and fast ($\sim$1.8) SW than in the gradual SEP events (3.5–4) of Reames (1998) and is also less step-like. Even with the better agreement between SEP

Figure 1. Ratios of the average 5 to 12 MeV nucleon^{-1} gradual SEP elemental abundances of Reames (1995, 1999) to the photospheric abundances of Lodders (2003) as a function of elemental FIP. The FIP ratio of $\sim$2.5 is smaller than that of a similar comparison using the older Anders & Grevesse (1989) photospheric values. From Mewaldt et al. (2006, 2007a).

and slow SW abundances, several elements such as He, C, and S were higher and Ne, N, and Mg were lower in the slow SW than in gradual SEP events.

2.2.2. Suprathermal Ions as Seeds

Measurements of SEP heavy-ion abundances over an extensive (0.1 to $>$60 MeV nucleon^{-1}) energy range became available with the 1997 launch of the *Advanced Composition Explorer (ACE)* satellite. Surveys of SEP abundances at $\sim$0.5 MeV nucleon^{-1} revealed the presence of enhanced ^{3}He/^{4}He ratios (Desai et al. 2001, 2006b), as well as a wide presence of He$^+$ ions (Kucharak et al. 2003), inconsistent with an SW seed population (Desai et al. 2006a). The tracer ion He$^+$ is present at 1 AU as a pickup ion and becomes highly enriched relative to He^{2+} above about $2 \times v_{sw}$, and ^{3}He is produced only in impulsive SEP events (Mason et al. 2005). In an earlier survey of 72 shock events, Desai et al. (2003) found significant correlations of elemental abundances between shock SEPs and shock ambient

upstream suprathermal ($E \gtrsim 0.1$ MeV nucleon^{-1}) populations. A systematic fractionation by A/Q of the shock SEPs compared with the upstream suprathermal population provided compelling evidence for a suprathermal seed population. Their study was recently extended (Allegrini et al. 2008) to show a systematic ionic A/Q shock SEP depletion for C-Fe and He$^+$ in comparison with the ambient suprathermal ion population upstream of each of 18 shocks. The shock SEP A/Q depletions prevailed even though the upstream suprathermal ions originated from different sources. With the additional lack of correlation between SW and shock SEP elemental abundances, Desai et al. (2003, 2006a) argued for suprathermals as seed particles. They noted that their speeds above theoretical injection thresholds and their isotropic velocity distributions make the suprathermals preferable to SW thermal ions as seed candidates for shock acceleration.
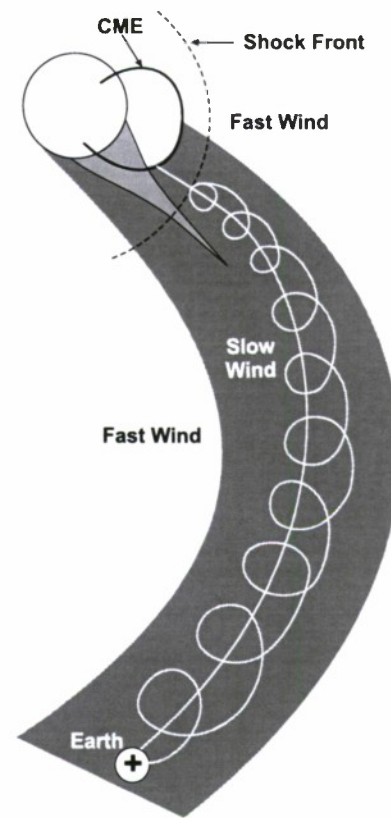
Additional support for an SEP suprathermal seed population has come from studies of quiet-time interplanetary suprathermal C/O and Fe/O and ^{3}He/^{4}He ratios between 0.04 and 1 MeV nucleon^{-1}, which were found to be similar at solar maximum to those of ions accelerated in SEP events and at solar minimum to thermal SW and corotating interaction region (CIR) ions (Desai et al. 2006b). That result was confirmed by additional studies of the same $\sim$20–160 keV nucleon^{-1} suprathermal ratios in 2102 transient upstream events near the Earth's bow shock (Desai et al. 2006d) and in selected quiet periods through the last solar cycle (Dayeh et al. 2009).

A detailed study of 64 large SEP (LSEP) events at 0.5–2 MeV nucleon^{-1} showed about half the events to have ^{3}He/^{4}He ratios enhanced by factors of 2–150 over the SW values (Desai et al. 2006c, 2007). The $E \sim 0.38$ MeV nucleon^{-1} heavy ion abundance enhancements with increasing A/Q were not systematically organized by slow SW abundances of von Steiger et al. (2000) or by the average 5–12 MeV nucleon^{-1} SEP abundances of Reames (1995, 1999), but they were remarkably similar to those observed in IP shock and ^{3}He-rich SEP events. The simultaneous enhancements of ^{3}He, with an A/Q lower than that of ^{4}He, and of heavy ions such as Fe, with an A/Q higher than that of O, precluded a rigidity-dependent acceleration of ambient SW material. Desai et al. (2006c, 2007) considered remnants from impulsive flares or gradual SEP events, as well as the suprathermal ions at $\sim$2–10 $\times v_{sw}$ as candidate seed populations. A current frustration is that for gradual SEP events, which are formed well inside 1 AU (Mason et al. 2005; Desai et al. 2006a), we can measure neither the shock properties nor the local seed populations.

2.2.3. Alternative Seed Populations

Alternatives to and limits of suprathermal seed populations for SEPs have also been considered. Mewaldt et al. (2006) calculated that the remnant flare suprathermal Fe densities were too low by a factor of $\sim$50 to account for the Fe SEPs over 0.04 keV $< E <$ 120 MeV nucleon^{-1} in LSEP hybrid events, defined by the presence of ^{3}He and/or Fe with $Q \geqslant 16$. The flare suprathermals were adequate, however, to provide seeds for the $E > 10$ MeV nucleon^{-1} portion of the spectra (Mewaldt et al. 2003; Tylka et al. 2005). Acceleration of an Fe-rich seed population from previous gradual SEP events or from ubiquitous suprathermal tails and a rigidity-dependent injection/acceleration mechanism favoring (contrary to IP shocks) heavy ions with large A/Q ratios were two suggested possibilities for $E \lesssim 10$ MeV nucleon^{-1} events.

Another interesting seed possibility is interplanetary CME (ICME) material (Mewaldt et al. 2006), which often has high Fe
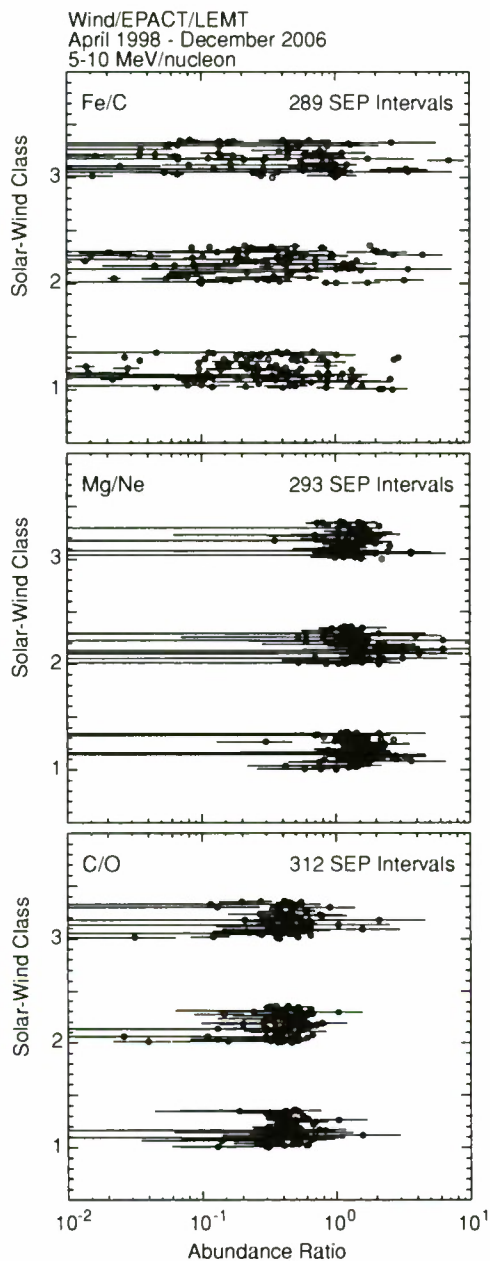

Figure 2. Diagram showing an SEP gyrating along a spiral magnetic field line in a slow SW region as it propagates from the Sun to the Earth. The dashed line shows a CME-driven shock extending into both slow and fast SW regions. We assume that SEPs observed in either slow or fast SW regions are shock accelerated in the same regions near the Sun. The SEPs and corresponding shock seed populations will be observed simultaneously at 1 AU. From Kahler & Reames (2003).

charge states and anomalous abundances. The SW is more Fe-rich and C-poor, in better agreement with SEP abundances, when the freeze-in temperatures, as measured by the SW O^{+7}/O^{+6} ratios, are higher. Selecting all 2 hr averages of SW composition in 2001 and 2003 with freeze-in temperatures >2 MK, which is predominately ICME material, Mewaldt et al. (2007a) found an SW FIP ratio of $\sim$5 based only on low-FIP Mg, Si, and Fe and high-FIP O. That FIP factor is not only well above those of the fast ($\sim$1.3) and slow ($\sim$1.7) SW but is similar to those of the 64 LSEP events of Desai et al. (2006c) and the 14 LSEP events ($\sim$3–3.5) of Cohen et al. (2007).

An extensive survey of >200 ICMEs by Richardson & Cane (2004, hereafter RC04) showed that SW values of He/H > 0.06 were predominately confined to ICMEs. They also found that while Mg/O and Ne/O ratios were generally anticorrelated with SW speeds, an enhancement by a factor of $\geqslant 2$ above those average values was a good indicator of ICME regions. From the best fits of their Figures 2 and 3 and for a typical SW speed of 400 km s^{-1}, these values would be Mg/O > 0.23 and Ne/O > 0.30. From these limits, Mg/Ne $= \sim$0.77. Reinard (2008) used a list of ICMEs updated from those of RC04 to examine He/H, Ne/O, and Mg/O ratios as functions of the ICME associated flare magnitudes, solar source longitudes, and magnetic structures. The ratios were biggest for the largest flares, central meridian sources, and magnetic clouds. If we take the ratios from the 43 central longitude ICMEs in her Table 2 (He/H $= 0.062 \pm 0.004$, Ne/O $= 0.34 \pm 0.02$, and Mg/O $= 0.32 \pm 0.03$) or the 41 magnetic clouds of her Table 5 (He/H $=$

Wind/EPACT/LEMT
April 1998 - December 2006
5-10 MeV/nucleon

Figure 3. Fe/C (top), Mg/Ne (middle), and C/O (bottom) ratios at 5 to 10 MeV nucleon^{-1} for each of the three SW types, where 1 is ICME, 2 is fast wind, and 3 is slow wind. The data points are spread out vertically within each group to show the ranges of variation.

0.065 ± 0.004, $Ne/O = 0.30 \pm 0.02$, $Mg/O = 0.28 \pm 0.02$), we get $He/H = 0.063 \pm 0.004$ and $Mg/Ne \sim 0.94 \pm 0.03$ as upper limits to the ICME values.

2.2.4. Coronal Thermal Ions Reconsidered as Seeds

Determining the abundances of the seed populations and their event-to-event variations from the SEP event measurements is complicated by the energy dependence of elemental ratios (Tylka et al. 2005; Mewaldt et al. 2007b). Cohen et al. (2007) selected 14 LSEP events in the <0.5 to >30 MeV nucleon^{-1} range with well determined power-law spectra and spectral rollovers and assumed elemental charge states and a spectral scaling to deduce energy-independent event abundances. They confirmed earlier results that the FIP ratio varies by about a factor of 2 among SEP events. They found that their 14 SEP-

event abundance averages did not agree well with either the coronal abundances of Feldman & Widing (2003) or the slow SW abundances of von Steiger et al. (2000), and they also pointed out poor agreement between slow SW and coronal abundances. Mewaldt et al. (2007a) selected a different set of 14 SEP events in the 12–40 MeV nucleon^{-1} range with little Q/A-dependent fractionation and with spectral slopes near the species mean slopes to get unbiased relative abundances of 10 elements. They found an average high-FIP depletion factor of ~ 4.6 compared with the photospheric abundances of Lodders (2003), and their 10 average elemental abundances at 12–40 MeV nucleon^{-1} were all consistent within 20% of the coronal abundances of Feldman & Widing (2003).

The Mewaldt et al. (2007a) result has therefore provided support for the contention of Reames (1995, 1999) that SEP abundances, properly deduced from the observations, can yield coronal abundances. The presence of ^3He and He^+ in some gradual SEP events (Mason et al. 2005) has made clear that flare remnants and pickup ions are important contributors to SEP seed populations, but the significant differences between coronal and SW abundances (Cohen et al. 2007) and FIP ratios (Mewaldt et al. 2007a) may not have been properly appreciated as SEP and SW abundance comparisons were made prior to the more recent coronal (Feldman & Widing 2003) and photospheric (Lodders 2003) abundance results.

If the acceleration mechanism of CIRs is similar to that of the gradual SEPs, then recent abundance measurements in CIRs (Mason et al. 2008) could be consistent with SW thermal ions as a primary seed population. The CIR elemental spectral forms were similar over a wide intensity range, and their abundance variations were minimal, making those measurements ideal for deducing the seed populations. Except for He^+ and ^3He, abundantly produced as pickup ions and flare SEPs, respectively, the CIR abundances at 320–450 keV nucleon^{-1} were very similar to the SW thermal abundances measured 2 to 4 days earlier. The observed CIR and SW thermal abundance similarities could result if the SW suprathermal abundances were in the same proportion to their thermal abundances for each element. This possibility flows from the recent mechanism of Fisk & Gloeckler (2006, 2007, 2008) that produces a ubiquitous low-energy power-law tail and high-speed cutoff by stochastic acceleration in SW thermally isolated compressional turbulence. However, at the current time we do not have suprathermal elemental abundances adequately determined for a comparison with gradual SEP abundances.

2.3. SW Abundances

If the seed populations for gradual SEP events originate in quiet coronal regions, then we might expect little compositional variation between the SEP events observed at 1 AU in fast SW regions and those in slow SW regions. On the other hand, SEP acceleration primarily in SW streams could yield abundance variations based on differences between the thermal or suprathermal compositions in those streams. The abundance composition differences between the ICMEs (Mewaldt et al. 2007a) and the fast and slow SW suggest that SEP abundances may differ among all three SW stream types.

To carry out our comparison of SEP elemental abundances in different SW stream types we first present in Table 1 the most recent elemental compositional data for the quiet corona and SW streams. This topic is complicated by the fact that different data sets have been used by different investigators for their comparisons. The photospheric abundances of Anders & Grevesse

Table 2
SEP and SW Elemental Abundance Ratios in SW Streams

Source	Solar Wind/SEP type	Mg/Ne[a]	Fe/C[b]	C/O[c]	He/H[d]
This Study					
	SEPs in Transients (1)[e,f]	1.402 ± 0.047	0.292 ± 0.031	0.418 ± 0.009	NA
	SEPs in Fast wind (2)[e,f]	1.482 ± 0.066	0.270 ± 0.036	0.433 ± 0.013	NA
	SEPs in Slow wind (3)[e,f]	1.423 ± 0.052	0.271 ± 0.043	0.439 ± 0.017	NA
	SEPs, all SW classes[e,f]	1.434 ± 0.032	0.270 ± 0.021	0.428 ± 0.007	NA
Previous Gradual SEP Studies (all SW classes)					
	Reames (1995)[e,g]	1.289 ± 0.043	0.288 ± 0.010	0.465 ± 0.009	0.0363 ± 0.0054
	Slocum et al. (2003)[j]	1.81 ± 0.28	0.31 ± 0.04	0.53 ± 0.04	NA
	Desai et al. (2006c)[h]	1.507 ± 0.046	1.119 ± 0.135	0.361 ± 0.012	NA
	Desai et al. (2006c)[i]	1.502 ± 0.041	0.798 ± 0.094	0.355 ± 0.009	NA
Other Sources					
	Coronal Above AR	1.17	0.380	0.490	0.085
	Bochsler Slow Wind[k]	1.05 ± 0.58	0.179 ± 0.092	0.680 ± 0.070	0.045[l]
	Bochsler Fast Wind[k]	0.76 ± 0.52	0.129 ± 0.087	0.680 ± 0.070	0.01–0.04[l]
	SWICS Fast Wind[m]	1.52 ± 0.52	0.094 ± 0.020	0.710 ± 0.080	—
	RC04 ICMEs	∼ 0.77	—	—	> 0.06
	Reinard ICMEs	0.94 ± 0.03	—	—	0.063 ± 0.004

Notes.

[a] FIP ratio low/high, rigidity ratio $\sim$ 1

[b] FIP ratio low/high, rigidity ratio $\sim$ 0.56

[c] FIP ratio high/high, rigidity ratio $\sim$ 0.9

[d] FIP ratio high/high, rigidity ratio $\sim$ 0.5

[e] Errors bars are statistical uncertainties in the mean values.

[f] at 5–10 MeV nucleon^{-1}

[g] at 5–12 MeV nucleon^{-1}, except He/H at 1–4 MeV nucleon^{-1}

[h] 64 events from 1997–2005, at 0.32–0.45 MeV nucleon^{-1}, with linear averaging of event-integrated values

[i] 64 events from 1997–2005, at 0.32–0.45 MeV nucleon^{-1}, with logarithmic averaging of event-integrated values

[j] 24 events from 1998–2002 with ^{3}He/^{4}He < 2% at 0.5–2.0 MeV nucleon^{-1}; heavy-ion measurements at 11.0–21.8 MeV nucleon^{-1}

[k] Error bars are the one-sigma statistical variations among daily-averages (von Steiger et al. 2000) plus systematic uncertainties (Bochsler 2007).

[l] estimated from Kasper et al. (2007)

[m] According to Gloeckler & Geiss (2007), error bars are mostly systematic uncertainties.

(1989) and Grevesse et al. (1996) used by Reames (1995, 1999) have been updated by the recommended photospheric values of Lodders (2003), which we use in Figure 1 and present in Table 1, after converting from her astronomical scale based on log n(H) = 12 to the O = 1000 abundance scale more useful for SEP abundance comparisons.

To compare SEP abundances with those in the corona, we also give the spectroscopic coronal abundances above typical quiet regions (at $\sim$1.4$\times$ 10^6 K and converted from the log n(H) = 12 scale) presented by Feldman & Widing (2003). The paradigm for SEP production at CME-driven shocks assumes that the SEP seed population occupies overlying open coronal/heliospheric regions rather than those lower quiet regions. Nevertheless, Cohen et al. (2007) and Mewaldt et al. (2007a, 2007b) found better agreement of their $0.1 \leqslant E \leqslant 100$ MeV nucleon^{-1} gradual SEP event abundances with those quiet coronal abundances than with either fast or slow SW abundances. However, the quiet coronal FIP ratios observed in equatorial streamers are known to increase with time (Feldman & Widing 2007), and may also increase from higher-density magnetically closed to lower-density open structures, which may be the sources of the slow SW (Ko et al. 2008).

The fast and slow SW elemental abundances of von Steiger et al. (2000) were the basis of the SEP abundance comparisons discussed above. Their values are derived from the Solar Wind Ion Composition Spectrometer (SWICS) on the *Ulysses* spacecraft and normalized to O. However, even here, there is some confusion since their Table 1 presented "Max" and "Min" values for the slow SW and "South" and "North" polar values for the fast SW. One must select one of the two sets of values or combine them for use in SW comparisons. Bochsler (2007) has recently compiled SW elemental abundances from various sources, normalized to O = 1, for both slow (interstream) and fast (coronal hole) SW streams, which are presented in the seventh and eighth columns of Table 1.

The elemental abundances of Gloeckler & Geiss (2007) for fast SW streams between 700 and 800 km s^{-1} from polar holes using *Ulysses* SWICS data are given in the last column. Each of their elemental abundances is given only for the most abundant isotope, so the total elemental values for all isotopes will be slightly higher. The biggest difference from the Bochsler (2007) fast SW stream values is that of Ne, for which the Gloeckler & Geiss (2007) value is a factor of $\sim$2 lower. Analysis of SW elemental abundance data from the NASA *Genesis* mission is not yet complete (Reisenfeld et al. 2007), but promises to be the standard for future work.

3. DATA ANALYSIS

3.1. SEP Magnetic Connection To Shocks

With measurements at 1 AU, we want to compare abundances of SEPs produced in near-solar shocks in slow SW regions versus shocks in fast SW regions. As the SW flows antisunward, it draws out the embedded magnetic field into the familiar

Parker spiral configuration, as shown in Figure 2. Reames (1995) explains the relationship between SEPs and SW plasmas at 1 AU as follows: "In a gradual event, particles are accelerated from the local plasma where the shock crosses the observer's field line. For quiescent conditions, the solar wind plasma along a given field line has emerged from the same point at the top of the corona, although the plasma near Earth emerged ~4 days prior to its arrival at 1 AU. Thus energetic-particle and solar-wind abundances share a common spatial origin but differ in the time of the sample. Only one spot on the Sun is viewed at a time; this spot is swept eastward across the disk as the observer moves to new field lines because of solar rotation." See also Figure 3.7 of Reames (1999).

An important assumption we add to this explanation is that there is minimal spreading of field lines and SEPs across the boundaries between the fast and slow SW regions. Thus SEPs observed in fast or slow SW regions at 1 AU are assumed to have been accelerated in shocks in the sunward extensions of the same regions. This picture may explain the results of a comparison by Mewaldt et al. (2006) between nine SEP events with enhanced $12 < E < 40$ MeV nucleon^{-1} Fe/O ratios and periods of suprathermal $E > 0.04$ MeV nucleon^{-1} Fe/O ratio observations. They assumed that suprathermal seed ions take ~1 day to reach 1 AU and reflect conditions near the Sun ~2 days earlier. However, the suprathermal Fe/O ratios on days before the SEP events were not unusually Fe-rich, but during the SEP events the suprathermal Fe/O ratios were much higher than normal. This is consistent with Figure 1, in which both the candidate seed population and the SEPs are confined to the same SW stream and are measured simultaneously at 1 AU. We note that the Mason et al. (2008) comparison between CIR ion abundances and SW thermal ions also used inappropriate 2 to 4 day earlier SW abundance measurements. They did find a good correlation between the CIR and SW abundances for Fe/O, but not for ^{3}He or He$^+$ enhancements.

3.2. Selection of SEP Events and SW Streams

We started with a list of 227 SEP events compiled from all Wind Energetic Particle Accleration, Composition and Transport (EPACT) 20 McV SEP proton enhancements of at least twice the background over the period from 1998 to the end of 2006. We first deleted probable impulsive SEP events, events of possible non-solar origins, or periods of LEMT data gaps. Unlike Kahler & Reames (2003) and Kahler (2004), we did not consider CME or flare associations. For each SEP event we then used data from the LEMT in the EPACT experiment (von Rosenvinge et al. 1995) on *Wind* to select for analysis times. An important advantage of the LEMT is its large geometric factor of 17 cm^2 sr for each of three identical detectors.

Richardson et al. (2002) classified SW observations since 1972 into three components as: (1) transient structures, including ICMEs, shocks and postshock flows; (2) fast SW streams; and (3) slow SW streams. Various SW signatures were used to identify the stream types, but they did not include ion charge states or elemental abundances (Cane & Richardson 2003). Richardson & Cane (2004) compared their list of 1996–2002 ICME periods (Cane & Richardson 2003) with ICME periods based on *ACE* SWICS SW compositional data over the same period and found good agreement. They concluded that their published list included at least ~90% of the ICME periods determined from the compositional data. Their list of ICMEs was then revised to include the SWICS compositional data (Richardson & Cane 2005), and is posted at

http://www.ssg.sr.unh.edu/mag/ace/ACElists/ICMEtable.html. The classification of the SW into the three stream components has been updated and used in our analysis (Richardson, private communication).

The selected 227 SEP event time periods were compared with the time periods of the component SW structures, and each SEP event was then divided into separate time segments, usually 1 to 3 in number, each corresponding to a single SW type. The total number of SEP time segments was 325, with four in category 0 (uncertain), 128 in 1 (transient), 101 in 2 (fast wind), and 92 in 3 (slow wind). The distributions of the total numbers of hours of the SEP time periods by SW types is 5368 (43%), 3823 (31%), 3175 (26%) in types 1, 2, and 3, consecutively. This is in rough agreement with total SW types 1, 2, and 3 distributions of ~35%, ~35%, and ~30% observed near solar maxima (Richardson et al. 2002).

We selected four SEP elemental ratios in fixed energy ranges for analysis. The Mg/Ne and Fe/C ratios match low-FIP (<9 eV) to high-FIP (>9 eV) elements. We also compared two pairs of abundant high-FIP elements, He/H and C/O. For temperatures of $1-2 \times 10^6$ K, $Q/A \sim 0.4$ for both Mg and Ne, while $Q/A \sim 0.27$ for Fe, ~ 0.41 for O, and ~ 0.48 for C (Reames 1999). Thus, for these charge states, the rigidity ratios for Mg/Ne and C/O are both ~1, while the rigidity ratios of Fe/C and He/H are both ~2. We calculated the abundance ratios of Mg/Ne, Fe/C, and C/O at 5–10 MeV nucleon^{-1} and of He/H at 2.1–2.5 MeV nucleon^{-1} for each of the 321 SW time intervals, similar to the energy intervals used by Reames (1995, 1999) in his abundance compilation.

3.3. Compositions of SEPs and SW Streams

Figure 3 demonstrates how the Fe/C, Mg/Ne, and C/O ratios vary in the three SW classes. Table 2 gives the unweighted averages of these ratios for each of the three SW types, as well as the averages for the combined sample of all three SW types. Since the Fe/C values range over more than an order of magnitude, we have calculated their averages logarithmically. For consistency, we have used this same method for the other ratios. In calculating the average heavy-ion abundance ratios, we required that the interval-averaged C intensity exceed 10^{-6} (cm^2 sr s MeV nucleon^{-1})$^{-1}$ so as to avoid time periods with insufficient ion statistics or potentially significant contamination from anomalous cosmic rays. This cut removed 17% of our time intervals. In the time intervals that passed this cut, He/H and C/O ratios were obtainable for all of them, while the number of intervals in the various SW classes with undetermined Mg/Ne or Fe/C ratios ranged from 0 to 3.6%. These unmeasured intervals were too few in number to cause significant systematic uncertainty in the values in Table 2. In particular, when we recalculated the mean values after assigning to each unmeasured interval the lowest abundance ratio observed in that sample of intervals, the mean values were unchanged to within the error bars given in Table 2.

While we find that the SEP He/H ratios do not vary significantly among the three SW stream types, instrumental effects in the LEMT have not allowed us to obtain absolute values of He/H, so they are listed in Table 2 as NA.

We also show in Table 2 abundance ratios from previous reports on gradual SEPs, as well as results from coronal and SW studies. The SEP values from Reames (1995, 1998) were measured at energies similar to ours. The Mg/Ne, Fe/C, and C/O averages in our combined sample of all three SW types agree with the corresponding results from Reames (1995) to within

~2.7, ~0.4, and ~3.2 standard deviations, respectively. These numbers suggest that the small discrepancies from Reames (1995) primarily reflect systematic differences in the averaging methods. Slocum et al. (2003) focused on smaller events from 1998–2002 and reported averages at 11.0–21.8 MeV nucleon^{-1}. Their averages thus have larger statistical uncertainties and are consistent with our results and Reames (1995) to within one or two standard deviations. Desai et al. (2006c) reported abundance ratios in 64 large gradual events from 1997–2005 at energies more than an order of magnitude smaller than ours. Their average Mg/Ne is slightly larger than ours, while their C/O is somewhat smaller. There is a very large difference in the average Fe/C ratios, with the lower-energy result higher than ours by a factor of three or four.

A technical issue arises in comparing to the Desai et al. 2006c values. Starting from an ensemble of measurements, the average abundance ratio can be calculated in two ways, either from the measurements themselves or from their logarithms. The linear method may seem more natural; but for a very wide distribution that spans more than an order of magnitude, we believe that the logarithmic averaging better characterizes the distribution. For this reason, we have used logarithmic averaging for the abundance ratios reported in this study. Desai et al. (2006c), however, used the linear averaging method, the results of which are shown in Table 2. To facilitate comparison with our results, we have also applied logarithmic averaging to the Desai et al. data. As seen in Table 2, for a compact distribution, such as found for C/O and Mg/Ne, the two different averaging methods give nearly identical results. But for a broad distribution, such as Fe/C, the results are quite different. The average Fe/C value from the Desai et al. study is closer to our average when calculated with the same method as ours.

The standard deviations in Table 2 are calculated from those given by the authors of each of the elemental abundance sources. The standard deviations on the SEP results are statistical uncertainties in the mean values, whereas the standard deviations on SW values represent one-sigma statistical variations among ~ daily averages (von Steiger et al. 2000) plus systematic uncertainties (Bochsler 2007; Gloeckler & Geiss 2007). No standard deviations for the coronal abundances were given by Feldman & Widing (2003).

The SW He/H ratio increases with SW speed, but that relationship also varies with solar cycle, with a larger range of ratios around cycle minimum and narrower range at cycle maximum (Kasper et al. 2007). We give crude estimates from Figure 1 of Kasper et al. (2007) for He/H in fast and slow SW. The ICME ratios of RC04 and Reinard (2008) were discussed in Section 2.2.3. Although Mewaldt et al. (2007a) showed that SW with high O^{+7}/O^{+6} ratios, characteristic of ICME SW, has decreased C/O and increased Fe/O ratios, they did not separately examine SW Fe/C ratios to get a range of those values for ICMEs. We believe that ICME Fe and C abundances or ratios have not been reported.

For each of the SW classes, our SEP averages are based on ~100 time intervals. The standard deviations of our SEP results may therefore be multiplied by ~10 to get a sample-variation analogous to that reported for the SW results. After doing this, the SEP and SW variations for Mg/Ne and C/O are seen to be comparable. The sample-variation in the SEP Fe/C, on the other hand, is two to four times larger than that of the SW Fe/C. The larger variability among SEP Fe/C values probably reflects transport distortions arising from these two ions' different charge-to-mass ratios (Ng et al. 1999; Tylka et al.

1999; Mason et al. 2006). Variations in the suprathermal seed population may also play an important role (Desai et al. 2006b, 2006c, 2006d).

The primary result of Table 2 is that the four selected SEP abundance ratios show no significant differences among the three SW types. We select periods in 2006 December and 2005 July–August that illustrate this relative insensitivity to the SW stream type. Figures 4 and 5 show the SW speed and O^{+7}/O^{+6} ratio as indicators of SW type in the lower panels and the SEP intensities and abundance ratios in the top panels. Despite large changes in the SW, the abundance ratios change only slowly, with the exception of the possible transport effects on Fe/C, as seen in Figure 5.
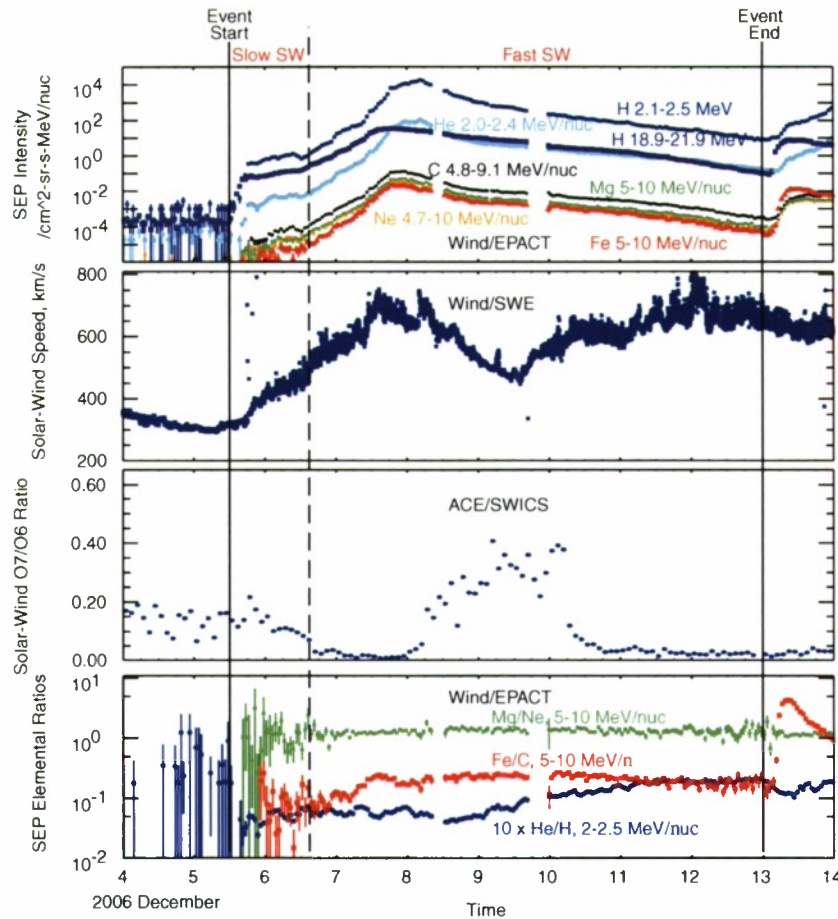
If we assume that the composition of the 5–10 MeV nucleon^{-1} SEP seed populations in the inner heliosphere varies among the SW types, then the most likely coronal/SW seed population of Table 2 would be that best matching our SEP ratios. Systematic uncertainties in the SW values do not allow us to make definitive conclusions, but we note several points. The SEP C/O averages are significantly lower than those of the SW averages, even though there is comparatively little variability within each. The SEP Fe/C ratios exceed both fast SW ratios of Table 2 and lie between the AR coronal and slow SW values, so the slow SW appears favored in this case. Because of the significant disparity of the Boehsler et al. (2007) and *Ulysses* SWICS fast SW values, the SEP Mg/Ne ratios exceed the first and are close to the second. However, the *Ulysses* values pertain only to SW with speeds of 700 to 800 km s^{-1}, which occurs predominately at high ecliptic latitudes, so those SW ratios are less likely to be source regions of the SEPs measured by EPACT in the ecliptic plane. Comparing only with the Bochsler et al. SW values, both the SEP Mg/Ne and Fe/C ratios are in better agreement with the slow than with the fast SW values. We are reluctant to compare our SEP Mg/Ne ratios with the ICME ratios of RC04, because we have derived that value by taking the ratio of their lower limits of Mg/O and Ne/O, which is also slightly dependent on the SW velocity. Finally, the Reames (1995) He/H ratio accords better with the broad range of the fast SW than with the higher value of the slow SW (Kasper et al. 2007).

3.4. SW Variation of SEP Energy Spectra and Intensities

We have computed the unweighted averages of the power-law energy exponents for minor ions and plotted those for each of the three SW types in Figure 6. The 3–10 MeV nucleon^{-1} Fe spectral indices are significantly harder than the other ions in all cases, but the reason for this is not understood. To optimize the statistics for the spectral fits, we included O rather than Mg, Ne, and C, which were used in the composition analysis of Table 2. The primary result here is that, as in the case of the elemental abundances, we find no energy spectral differences among the three stream types.

For each of the ions and each SW time interval we calculated the time-averaged ion intensity. Then we calculated the unweighted averages of those intensities for each SW stream type. Figure 7 shows the plot of the unweighted time-averaged intensities of each element for each SW type. In contrast to the composition and energy spectra comparisons, we do find that the intensities in SW type 1, the ICME periods, are significantly enhanced above those of the fast and slow SW streams. There is no significant intensity difference between the latter two SW streams.
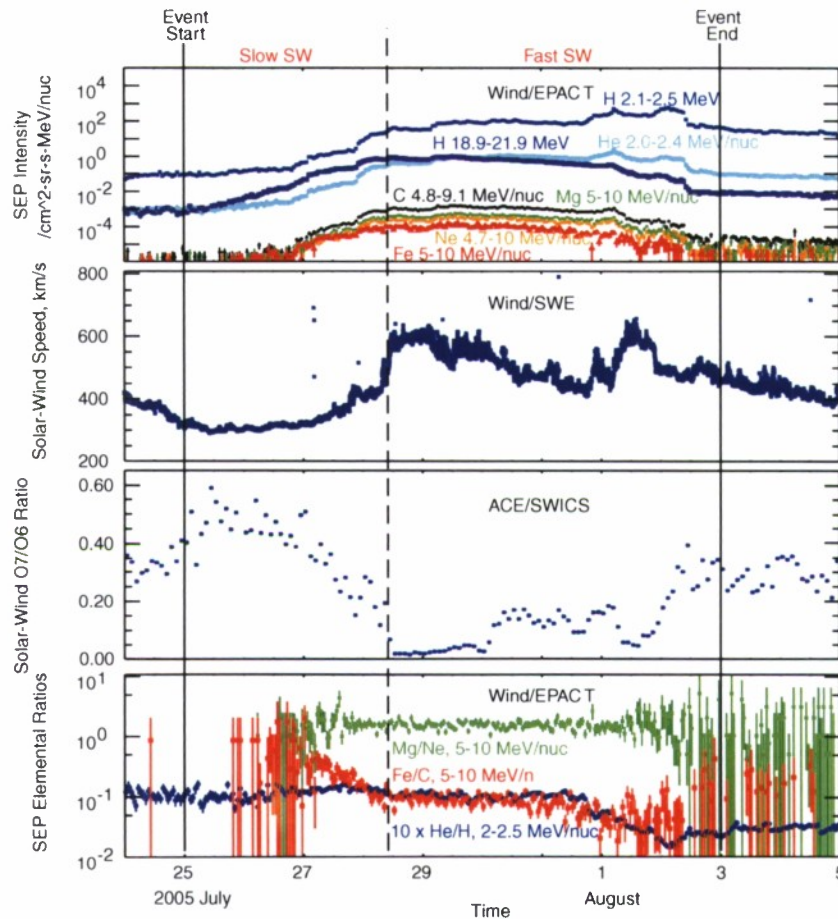
Figure 4. Example of an SEP period in December 2006 when the SW stream structure changed from slow (SW3) to fast (SW2) structures. Vertical lines show the boundary in the SW stream structures and the beginning and end of the periods used for SEP abundance ratios. The top panel shows intensity-time profiles of 2 and 20 MeV H along with the 5–10 MeV nucleon^{-1} profiles of high-FIP elements C and Ne and low-FIP elements Mg and Fe. The middle panels show the inversely correlated SW speeds and SW O^{+7}/O^{+6} ratios that indicate the changing stream structures. In the bottom panel the corresponding Mg/Ne ratio varies little throughout the SEP event. The Fe/C ratio has strong variation during the first day of the event but thereafter varies slowly and comparatively little. The 2–2.5 MeV nucleon^{-1} He/H ratio shows only slow variations over the time period. The period around 9 December shows a tendency toward slow wind (SW3) which is not separated by the RC04 criteria from the larger fast (SW2) stream. However, the low variance of the Mg/Ne and Fe/C ratios in that period is clear. A new SEP event begins on 13 December.
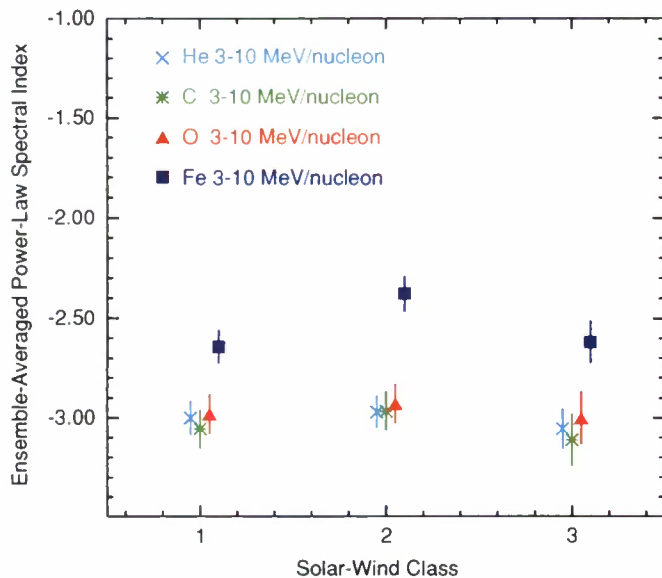
4. DISCUSSION

SW elemental composition has been shown to vary among the three types of SW streams (RC04, Mewaldt et al. 2007a), so we might expect that seed populations, whether thermal or suprathermal ions, for shock acceleration of SEPs would also have an SW stream-type dependence. If so, then those compositional differences should be reflected in the SEP populations produced and observed in those different streams. Here, we have segregated SEP events by SW stream type to look for stream-dependent differences in the averaged SEP properties. We find that the examined SEP composition ratios, which matched low/high (Mg/Ne and Fe/C) or high/high (C/O and He/H) FIPs, and similar (Mg/Ne and C/O) or different (Fe/C He/H) rigidities, are the same to within statistical uncertainties for all three SW stream types (Figure 3 & Table 2). These similarities occur despite the intrinsically large ranges in the abundance ratios of the individual SEP periods examined. The present analysis used only bulk properties of different SW stream types and does not rule out the possibility that a more direct comparison of SEP elemental composition with upstream SW composition on a case by case basis could yield significant SW–SEP abundance correlations. Such a correlation has recently been found by Allegrini et al. (2008) for ICME-driven shocks at 1 AU.

We compared the observed SEP abundance ratios with those reported for the corona over active regions and for the fast and slow SW. Good matches were not found for any of the SW stream abundances, but the slow SW gives a slightly better match than the transient SW for the SEP abundance ratios. Mewaldt et al. (2007a) have argued that the large FIP effect found in SEP events and in ICME SW makes the ICME material a likely SEP seed population. That argument was based on averages over many ICME periods and SEP events rather than on direct comparisons between individual SEP events and their associated ambient SW abundances. Unfortunately, the ICME SW elemental abundance ratios of RC04 and Mewaldt et al. (2007a) were not suitable for a direct comparison with our SEP abundance calculations, so we can not rule out a better match of the SEP abundances with ICME than with slow SW abundances. However, the primary result here is that SEP elemental composition is independent of the SW stream type. This result provides no guidance in the quest to determine the seed populations for the shock-driven SEP events.

The stream independence of the SEP events extends to their energy spectra as well. There are no significant differences in the spectral indices among the three SW streams (Figure 6). The time-averaged SEP intensities, however, were higher by a factor of 4 to 6 for the transient SW (Figure 7). We noted earlier that
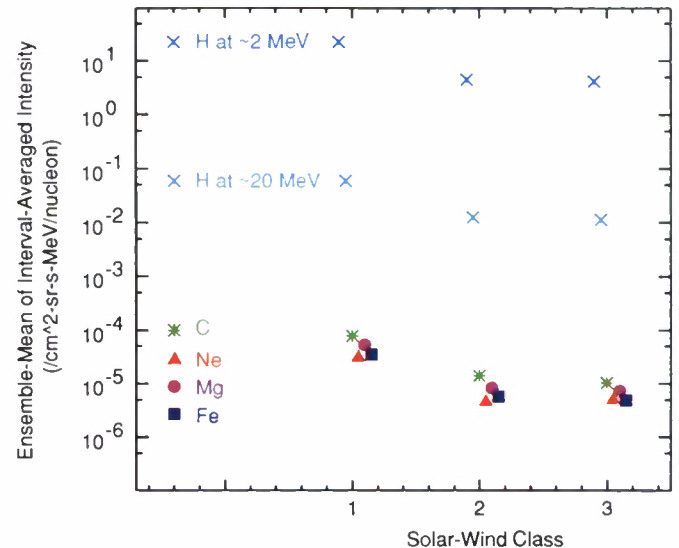
Figure 5. SEP period in 2005 July and August when the SW stream structure changed from slow (SW3) to fast (SW2) structures. Descriptors of the panels and vertical lines are similar to those in Figure 4. In the bottom panel, the corresponding Mg/Ne and the 2–2.5 MeV nucleon^{-1} He/H ratio vary little throughout the SEP event. The initial decline of the Fe/C ratios is probably a propagation effect due to their different ionic rigidities.

Figure 6. SEP event ensemble-averaged power-law spectral indices over the 3–10 MeV nucleon^{-1} ranges for the minor ions. The unweighted averages are plotted on an inverse scale for each of the three SW classes.

Figure 7. SEP event ensemble-averaged intensities for 2 and 20 MeV protons (H) and 5–10 MeV nucleon^{-1} Fe, Ne, C, and Mg for the transient (1), fast (2), and slow (3) SW streams. The intensities are significantly higher in the transient SW streams.

the SEPs occupy a slightly larger fraction (43%) of transient SW structures than would random time periods (~35%). This tendency for more intense and longer-lived SEP events to lie in transient SW regions may be expected since those regions are by

definition occupied by shocks, post-shock turbulence regions, and ICMEs. The production of SEP events is also enhanced when CMEs erupt into SW regions occupied by previous CMEs (Gopalswamy et al. 2004; Kahler & Vourlidas 2005).

Our finding of no significant SW-stream differences in 5–10 MeV nucleon^{-1} SEP elemental composition or energy spectra extends the results of Kahler & Reames (2003) and Kahler (2004), who found no differences between fast and slow SW regions for $E \sim 20$ MeV SEP event occurrences or peak intensities at 1 AU. They distinguished SW streams based only on the SW O^{+7}/O^{+6} ratios and did not separately consider transient SW streams, which would be a subset of the slow SW streams with the highest SW O^{+7}/O^{+6} ratios (RC04). The implication of their and our results is that if there are conditions for SEP production that systematically differ among the SW stream types, we have no evidence of such differences in the SEP elemental abundances at 1 AU. This could mean that several other variables are in play in the acceleration process. Lee (2007) has discussed three factors which determine the elemental composition of shock-accelerated SEPs. The first factor is the available seed population, for which the SW stream compositions do not seem a good match, as indicated in Table 2. At this point, suprathermal ions appear a most likely seed population candidate, but this has yet to be verified by the kind of direct comparisons done for IP shocks (Allegrini et al. 2008). The other two factors determining shock element abundances are the fractionation processes at both the seed-particle injection into the shock and the escape of the energetic ions from the shock region. The last two factors depend critically upon the magnetic obliquity of the shock. It is obvious that such processes and seed populations could vary substantially from shock to shock to produce the broad ranges of measured abundance ratios of Table 2. Finally we point out that substantial magnetic-field line wandering in the heliosphere (Ragot 2006) could result in cross-stream transport of SEPs or suprathermal seed particles, which would undermine the basic assumption of this study.

REFERENCES

Allegrini, F., Desai, M. I., Mason, G. M., Kucharek, H., & Mobius, E. 2008, ApJ, 682, 690
Anders, E., & Grevesse, N. 1989, Geochim. Cosmochin. Acta, 53, 197
Bochsler, P. 2007, A&AR, 14, 1
Cane, H. V., & Richardson, I. G. 2003, J. Geophys. Res., 108, 1156
Cohen, C. M. S., et al. 2007, Space Sci. Rev., 130, 183
Dayeh, M. A., et al. 2009, ApJ, 693, 1588
Desai, M. I., et al. 2001, ApJ, 553, L89
Desai, M. I., et al. 2003, ApJ, 588, 1149
Desai, M. I., et al. 2006a, Space Sci. Rev., 124, 261
Desai, M. I., et al. 2006b, ApJ, 645, L81
Desai, M. I., et al. 2006c, ApJ, 649, 470

Desai, M. I., et al. 2006d, Geophys. Res. Lett., 33, L18104
Desai, M. I., et al. 2007, Space Sci. Rev., 130, 243
Feldman, U., & Widing, K. G. 2003, Space Sci. Rev., 107, 665
Feldman, U., & Widing, K. G. 2007, Space Sci. Rev., 130, 115
Fisk, L. A., & Gloeckler, G. 2006, ApJ, 640, L79
Fisk, L. A., & Gloeckler, G. 2007, Space Sci. Rev., 130, 153
Fisk, L. A., & Gloeckler, G. 2008, ApJ, 686, 1466
Gloeckler, G. 2003, in AIP Conf. Proc. 679, Tenth Int. Solar Wind Conf., ed. M. Velli, R. Bruno, F. Malara, & B. Bucci (Melville, NY: AIP), 583
Gloeckler, G., & Geiss, J. 2007, Space Sci. Rev., 130, 139
Gopalswamy, N., Yashiro, S., Krucker, S., Stenborg, G., & Howard, R. A. 2004, J. Geophys. Res., 109, A12105
Grevesse, N., Noels, A., & Sauval, A. J. 1996, in ASP Conf. Ser. 99, Cosmic Abundances, ed. S. Holt & G. Sonneborn (San Francisco, CA: ASP), 117
Kahler, S. 2001, J. Geophys. Res., 106, 20947
Kahler, S. W. 2004, ApJ, 603, 330
Kahler, S. W. 2005, ApJ, 628, 1014
Kahler, S. W. 2008, Proc. 30th Int. Cosmic-Ray Conf. (Merida) 1, 143
Kahler, S. W., & Reames, D. V. 2003, ApJ, 584, 1063
Kahler, S. W., & Vourlidas, A. 2005, J. Geophys. Res., 110, A12S01
Kasper, J. C., Stevens, M. L., Lazarus, A. J., Steinberg, J. T., & Ogilvie, K. W. 2007, ApJ, 660, 901
Ko, Y.-K., Li, J., Riley, P., & Raymond, J. C. 2008, ApJ, 683, 1168
Kucharek, H., et al. 2003, J. Geophys. Res., 108, 8040
Lee, M. A. 2007, Space Sci. Rev., 130, 221
Lodders, K. 2003, ApJ, 591, 1220
Mason, G. M., et al. 2005, in AIP Conf. Proc. 781, The Physics of Collisionless Shocks, ed. G. Li, G. P. Zank, & C. T. Russell (Melville, NY: AIP), 219
Mason, G. M., et al. 2006, ApJ, 647, L65
Mason, G. M., et al. 2008, ApJ, 678, 1458
Mazur, J. E., Mason, G. M., Klecker, B., & McGuire, R. E. 1992, ApJ, 401, 398
Mewaldt, R. A., Cohen, C. M. S., & Mason, G. M. 2006, in Geophys. Mon. Ser. 165, Solar Eruptions and Energetic Particles, ed. N. Gopalswamy, R. Mewaldt, & J. Torsti (Washington, DC: AGU), 115
Mewaldt, R. A., et al. 2001, Proc. 27th Int. Cosmic-Ray Conf. (Hamburg), 8, 3132
Mewaldt, R. A., et al. 2003, Proc. 28th Int. Cosmic-Ray Conf. (Tsukuba), 6, 3229
Mewaldt, R. A., et al. 2005, in AIP Conf. Proc. 781, The Physics of Collisionless Shocks, ed. G. Li, G. P. Zank, & C. T. Russell (Melville, NY: AIP), 227
Mewaldt, R. A., et al. 2007a, Space Sci. Rev., 130, 207
Mewaldt, R. A., et al. 2007b, Space Sci. Rev., 130, 323
Ng, C. K., Reames, D. V., & Tylka, A. J. 1999, Geophys. Res. Lett., 26, 2145
Ragot, B. 2006, ApJ, 647, 630
Reames, D. V. 1995, Adv. Space Res., 15, 41
Reames, D. V. 1998, Space Sci. Rev., 85, 327
Reames, D. V. 1999, Space Sci. Rev., 90, 413
Reinard, A. A. 2008, ApJ, 682, 1289
Reisenfeld, D. B., et al. 2007, Space Sci. Rev., 130, 79
Richardson, I. G., & Cane, H. V. 2004, J. Geophys. Res., 109, A09104
Richardson, I. G., & Cane, H. V. 2005, in Proc. Solar Wind 11/SOHO 16, ed. B. Fleck, et al. (SP-592, Noordwijk: ESA), 154.1
Richardson, I. G., Cane, H. V., & Cliver, E. W. 2002, J. Geophys. Res., 107, SSH 8-1
Slocum, P. L., et al. 2003, ApJ, 594, 592
Tylka, A. J., Reames, D. V., & Ng, C. K. 1999, Geophys. Res. Lett., 26, 2141
Tylka, A. J., & Lee, M. A. 2006, ApJ, 646, 1319
Tylka, A. J., et al. 2005, ApJ, 625, 474
von Rosenvinge, T. T., et al. 1995, Space Sci. Rev., 71, 155
von Steiger, R., et al. 2000, J. Geophys. Res., 105, 27217